PSEUDO ELASTIC ANALYSIS OF MATERIAL NON-LINEAR PROBLEMS USING ELEMENT FREE GALERKIN METHOD

Raju Sethuraman* and Cherku Sridhar Reddy

ABSTRACT

Element Free Galerkin Method (EFGM) based on pseudo-elastic analysis is presented for the determination of inelastic solutions. In the proposed method a linear elastic analysis, using moving least square approximating function, is carried out for the determination of stress field of material non-linear problems using material parameters as field variables. Hencky's total deformation theory is used to define effective elastic material parameters, which are treated as spatial field variables and considered to be functions of equilibrium stress state and material properties. These effective material parameters are obtained in an iterative manner based on strain controlled projection method and total energy balance Neuber's rule, using experimental uniaxial tension test curve. The effectiveness of the method is illustrated using a problem of cylindrical vessel subjected to internal pressure and shear loads. Three different material models are considered for the problem: elastic-perfectly plastic, linear strain hardening type and nonlinear behavior obeying Ramberg-Osgood model. Obtained results for all the cases are compared with standard nonlinear finite element results and are found to be in good agreement.

Key Words: Element Free Galerkin Method (EFGM), pseudo elastic analysis, material non-linearity, effective material parameters.

I. INTRODUCTION

Due to the mathematical complexities involved in solving material non-linear problems, numerical methods are commonly employed. Analytical solutions are limited to simple geometry and boundary tractions. Extensively Finite Element Method (FEM) and boundary integral equation methods are used to solve boundary value problems. In recent years, meshless methods have become very promising, attractive and efficient numerical methods for solving boundary and initial value problems in the field of continuum mechanics. Meshless methods are increasingly become suitable for moving boundary value problems, especially for crack propagation problems, since nodes can be easily added or removed, which is other wise very tedious for mesh based methods like the finite element method. The discrete form of the continuum in the meshless method is basically obtained by using moving least square approximating functions for interpolant. No smoothing of stress or displacement field is needed, whereas for methods like finite element, one needs to perform smoothing of field variables across the inter element boundary to recover the best possible smooth results.

One of the earliest meshless methods is the Smooth Particle Hydrodynamics Method developed by Lucy (1977), which was used to model astrophysical phenomena. Later, Moving Least Square (MLS) approximations started gaining importance in meshless approximation procedures. Moving Least Square approximants were introduced and studied by Lancaster and Salkauskas (1981), originally for surface data fitting. Nayroles *et al*. (1992) introduced a method called Diffuse Element method that is essentially based on moving least square approximations. They used only a set of nodes and a boundary description for the development of the Galerkin equations and made element based mesh totally unnecessary.

Later, Belytschko *et al*. (1994) extended the applicability of EFGM based on MLS approximations

*Corresponding author. (Tel: +91-44-22578538; Fax: +91-44-22570509; Email: sethu@iitm.ac.in)

The authors are with the Department of Mechanical Engineering, Indian Institute of Technology Madras, Chennai-600 036, India.

to elasticity and heat conduction problems and showed that rate convergence can exceed that of finite elements significantly. Meshless methods are suitable for moving boundary value problems, especially for crack propagation problems, since nodes can be easily added or removed. Belytschko *et al.* (1995) illustrated the application of EFGM for an arbitrary crack growth problem. Belytschko *et al.* (1996) have presented an excellent overview of meshless methods, mainly focusing on kernel approximations, moving least square approximations and partitions of unity. Moving least square approximants' values are not equal to the nodal values since the shape function, in general, is not unity at that node. The nodal values are treated as fictitious nodal values. Hence, the essential boundary conditions have to be applied by the use of additional constraints in the form of Lagrange Multipliers or by using penalty parameters. Zhu and Atluri (1998) present a penalty formulation for easily enforcing the essential boundary conditions in the EFGM. Chen *et al*. (1996), presented the implementation of the reproducing kernel particle method for large deformation analysis of nonlinear structures. Later, Chen *et al*. (1998) extended the method for metal forming problems. Barry and Saigal (1999), and Xu and Saigal (1999) developed an elasto-plastic formulation, based on incremental theory, for solving crack growth in elasto-plastic materials using EFGM. The formulation is based on the consistent tangent operator approach. Recently, Liu (2002) wrote a book, which provides systematic steps that lead the reader to understand mesh free methods. Wang *et al*. (2002) solved Biot's consolidation problem using a radial point interpolation method. Rao and Rahman (2003) exploited the applicability of EFGM for calculating fracture parameters for a stationary crack in two-dimensional functionally graded materials.

Jahed *et al*. (1997) developed an analytical method to solve pressure vessel problems in the elasto-plastic range. In their method, the cylindrical pressure vessel was considered to be an assembly of a finite number of strips and a closed form elastic solution was used within each strip. The material properties are considered to be varying along the radial direction, but constant within the strips. The application of this method is restricted to problems for which the finite strip has closed form solutions. Babu and Iyer (1998) developed a robust method using the relaxation method, which is based on the GLOSS method of analysis. Here an attempt was made to satisfy force equilibrium in the plastic range. Recently, Seshadri and Babu (2000) extended the GLOSS method for determining inelastic effect in mechanical components and obtained conservative bounds for the determination of inelastic local strains. Desikan and Sethuraman (2000), proposed a pseudo elastic finite element method for the determination of inelastic whole field solutions. In this method linear elastic finite element analysis is carried out for solving elasto-plastic problems using constant strain triangular element. A similar approach is extended in the present paper for the determination of inelastic solutions using element free Galerkin method.

The objective of the present paper is to develop an Element Free Galerkin Method (EFGM) for solving inelastic problems based on a pseudo elastic solution. EFGM analysis coupled with pseudo elastic solutions will be carried out for solving elasto-plastic problems using material parameters as field variables. The method is based on Hencky's total deformation theory and will be restricted to proportional loading. Two algorithms, namely the projection method, and the Neuber rule, will be used to calculate the material parameters. The effectiveness of the method will be demonstrated using a pressure vessel subjected to internal pressure and shear loads for general hardening material behaviour.

II. METHODOLOGY

In this section, first the pseudo elastic analysis is briefly explained, followed by the element free Galerkin method (EFGM) and numerical implementation. In the analysis of static elasto-plastic problems, the weak form of the equilibrium equation is given as

$$\iiint_{\Omega} \sigma_{ij}\delta\varepsilon_{ij}d\Omega - \iiint_{\Omega} b_m\delta u_m d\Omega - \iint_{\Gamma_1} t_k\delta u_k d\Gamma + \iint_{\Gamma_2} \lambda(u_k - \overline{u}_k)\delta u_k d\Gamma = 0 \quad (1)$$

The essential conditions on Γ_2 are introduced in the above weak form of equilibrium equation using penalty parameter λ.

1. Stress-Strain Relationship in Terms of Effective Material Parameters

The strain-stress relationship for materials obeying total deformation theory of plasticity can be taken in the form

$$\varepsilon_{ij} = (\frac{1+\upsilon}{E} + \Phi)\sigma_{ij} - (\frac{\upsilon}{E} + \frac{1}{3}\Phi)\sigma_{kk}\delta_{ij} \quad (2)$$

where Φ is a scalar valued function used in Hencky's deformation theory and is given by

$$\Phi = \frac{3}{2}\frac{\varepsilon^p_{eq}}{\sigma_{eq}} \quad (3)$$

The equivalent plastic strain and the equivalent stress are defined as,

$$\varepsilon_{eq}^{p} = \sqrt{\frac{2}{3}\varepsilon_{ij}^{p}\varepsilon_{ij}^{p}} \quad \text{and} \quad \sigma_{eq} = \sqrt{\frac{3}{2}S_{ij}S_{ij}} \tag{4}$$

The deviatoric stress tensor is defined as

$$S_{ij} = \sigma_{ij} - \frac{1}{3}\sigma_{kk}\delta_{ij} \tag{5}$$

All the variables inside the parentheses of Eq. (2) are involved with the material properties, the final equivalent total plastic strain and the equivalent stress corresponding to equilibrium state. Eq. (2) can be written as

$$\varepsilon_{ij} = (\frac{1+\upsilon_{eff}}{E_{eff}})\sigma_{ij} - (\frac{\upsilon_{eff}}{E_{eff}})\sigma_{kk}\delta_{ij} \tag{6}$$

where, υ_{eff} and E_{eff} are the effective Poisson's ratio and effective Young's modulus respectively, which are functions of Young's modulus and Φ, and they are treated as material parameters. The effective material parameters are given as

$$\frac{1}{E_{eff}} = \frac{1}{E} + \frac{2}{3}\Phi \tag{7}$$

$$\upsilon_{eff} = E_{eff}(\frac{\upsilon}{E} + \frac{\Phi}{3}) \tag{8}$$

Using Eqs. (3) and (7) for elastic-perfectly plastic material E_{eff} is obtained as

$$\frac{1}{E_{eff}} = \frac{1}{E} + \frac{\varepsilon^{p}}{\sigma_0} \tag{9}$$

Similarly, for linearly work hardening material having tangent modulus E_T, the E_{eff} is obtained as

$$\frac{1}{E_{eff}} = \frac{\sigma_0}{E\sigma} + \frac{\sigma-\sigma_0}{\sigma E_T} \tag{10}$$

Substituting Eqs. (9) and (10) in Eq. (8) the effective Poisson's ratios for elastic-perfectly plastic and linearly hardening materials are obtained.
For the Ramberg-Osgood model,

$$\frac{\varepsilon}{\varepsilon_0} = \frac{\sigma}{\sigma_0} + \alpha[\frac{\sigma}{\sigma_0}]^{n} \tag{11}$$

the effective Young's modulus and the effective Poisson's ratio are obtained as

$$\frac{1}{E_{eff}} = \frac{1}{E} + \alpha\varepsilon_0[\frac{\sigma}{\sigma_0}]^{n-1}\frac{1}{\sigma_0} \tag{12}$$

$$\upsilon_{eff} = E_{eff}[\frac{\upsilon}{E} + \frac{1}{2}\alpha\frac{\varepsilon_0}{\sigma_0}[\frac{\sigma}{\sigma_0}]^{n-1}] \tag{13}$$

The effective material parameters are functions of the final state of stress fields. Hence, E_{eff} and υ_{eff} can be thought of as field variables describing the material properties at each point, since the final state of stress at every point is unique. Clearly, for constant values of E_{eff} and υ_{eff} Eq. (6) describes the elastic behaviour of the body. It is known that every state of stress at a point in the continuum, in equivalent sense, follows an experimental uniaxial stress-strain curve. From that point of view and from Eqs. (9), (10) and (12) the reciprocal of E_{eff} is nothing but a secant modulus defined on the experimental uniaxial curve. Hence the effective modulus can be obtained from the experimental material curve.

2. Moving Least Square Interpolant

In solving the equilibrium Eq. (1), the required displacement function $u(x)$ is approximated by the moving least square approximating function $u^h(x)$ in a sub-domain and is given as

$$u^h(x) = \sum_{i=1}^{m} P_i(x)a_i(x) \tag{14}$$

where $P_i(x)$ is a vector of complete basis functions (monomial basis) of order m and $a_i(x)$ are unknown coefficient functions. The coefficient vector function $a_i(x)$ is determined by minimizing a weighted discrete L_2 norm, which is defined as

$$J(x) = \sum_{j=1}^{n} w(x-x_j)[\sum_{i}^{m} P_i(x_j)a_i(x) - \hat{u}_j]^2 \tag{15}$$

where $\hat{u}_i$ are the fictitious nodal values and w_i is the weight function associated with the node i. After minimizing $J(x)$ with respect to coefficient functions $a_i(x)$ and appropriately rearranging the terms, the displacement function is obtained as

$$u^h(x) = \sum_{j=1}^{n} \varphi_j(x)\hat{u}_j \tag{16}$$

φ_i can then be described as the shape function associated with the nodes and is given as

$$\varphi_i(x) = \mathbf{p}^T(x)\mathbf{A}^{-1}(x)\mathbf{B}(x_i) \tag{17}$$

where,

$$\mathbf{A}(x) = \sum_{i=1}^{n} w(x-x_i)\mathbf{p}(x_i)\mathbf{p}^T(x_i) \tag{18}$$

$$\mathbf{B}(x) = [w(x-x_1)\mathbf{p}(x_1),\ w(x-x_2)\mathbf{p}(x_2),\ \cdots,\ w(x-x_n)\mathbf{p}(x_n)] \tag{19}$$

3. Weight Function

The weight function that has been used in the present study is quatric spline, which is expressed as a function of normalized radius r.

$$w(x-x_i)= 1-6r^2+8r^3-3r^4 \text{ for } r\le 1$$
$$=0 \qquad \text{for } r>1 \tag{20}$$

where, $r=d_i/d_{mi}$, in this $d_i=\|x-x_i\|$ is the distance from a sampling point x to a node x_i, and d_{mi} is the domain of influence of the node 'i'. The size of the domain of influence is computed by

$$d_{mi}=d_{\max}\mu \tag{21}$$

where μ is the scaling parameter, which is varied between 1.0 - 2.0. The distance $d_{\max}$ is determined by searching for enough neighborhood nodes so as to satisfy the regularity condition of $\boldsymbol{A}(x)$ (Eq.18) while determining shape functions. In the current study, for convenience, the elements that are generated by a finite element preprocessor using structured mesh are used as the background cells. Later, these cells are used for numerical integration of stiffness matrix. The vertices of the cells are made to coincide with the nodes. In order to find out the distance $d_{\max}$ for a particular node the following procedure is adopted; first the neighborhood cells attached to that node are identified. Then, nodes corresponding to those selected cells are noted, and the distance between these nodes and the considered node 'i' are calculated. The maximum distance of these is taken as $d_{\max}$ associated with the node 'i'.

4. Discrete Form of Equilibrium Equation

The discrete form of equations, using EFGM, can be obtained as in the standard Finite Element Method (FEM) using the weak form of equilibrium equations. Unlike in FEM, the direct imposition of the exact value of essential boundary conditions for the EFGM is always difficult because the shape functions derived from the Moving Least Square (MLS) approximation do not have the delta function property and nodal values are fictitious nodal values. Depending on the method that is used in enforcing the essential boundary conditions, the form of the discrete equations will change. In the present study, the essential boundary conditions are enforced by using a penalty approach (Zhu and Atluri, 1998).

The discrete equations that are obtained by using the penalty approach are presented here. At first, the MLS approximation $u^h(x)$ of the function $u(x)$ is rewritten in the global form for a two dimensional problem, as

$$\begin{Bmatrix} u_1 \\ u_2 \end{Bmatrix} = [\boldsymbol{H}]\{\hat{\boldsymbol{u}}\} \tag{22}$$

where, u_i is the displacement in X_i direction and

$$[\boldsymbol{H}]=[\boldsymbol{H}_1 \ \boldsymbol{H}_2 \ \boldsymbol{H}_3 \ \cdots \ \boldsymbol{H}_N] \tag{23}$$

$$\boldsymbol{H_i} = \begin{bmatrix} \varphi_i(x) & 0 \\ 0 & \varphi_i(x) \end{bmatrix} \tag{24}$$

$$\{\hat{\boldsymbol{u}}\}^T = [\hat{\boldsymbol{u}}_1 \ \hat{\boldsymbol{u}}_2 \ \hat{\boldsymbol{u}}_3 \cdots \hat{\boldsymbol{u}}_N] \tag{25}$$

$$\hat{\boldsymbol{u}}_i = [\hat{u}_i^1 \hat{u}_i^2] \tag{26}$$

where $\hat{u}_i^1$ and $\hat{u}_i^2$ are fictitious nodal displacements in X_1 and X_2 directions respectively for node $\boldsymbol{i}$, and N is the total number of nodes in the whole domain.

Substituting the trial function, Eq. (22), in the weak form of the equilibrium equation, Eq. (1), we get the following discrete equations

$$[\boldsymbol{K}]\{\hat{\boldsymbol{u}}\} = \{\boldsymbol{F}\} \tag{27}$$

where,

$$\boldsymbol{K} = \int_\Omega \boldsymbol{B}^T\boldsymbol{D}\boldsymbol{B}d\Omega + \lambda\int_{\Gamma_2} \boldsymbol{H}^T\boldsymbol{S}\boldsymbol{H}d\Gamma \tag{28}$$

$$\boldsymbol{F} = \int_\Omega \boldsymbol{H}^T\boldsymbol{b}d\Omega + \int_{\Gamma_1} \boldsymbol{H}^T\boldsymbol{t}d\Gamma + \lambda\int_{\Gamma_2} \boldsymbol{H}^T\boldsymbol{S}\overline{\boldsymbol{u}}\,d\Gamma \tag{29}$$

where,

$$\boldsymbol{B}=[\boldsymbol{B}_1 \ \boldsymbol{B}_2 \ \boldsymbol{B}_3 \ \ldots \ \boldsymbol{B}_N] \tag{30}$$

$$\boldsymbol{B}_i = \begin{bmatrix} \varphi_{i,1} & 0 \\ 0 & \varphi_{i,2} \\ \varphi_{i,2} & \varphi_{i,1} \end{bmatrix} \tag{31}$$

$$\boldsymbol{S} = \begin{bmatrix} S_1 & 0 \\ 0 & S_2 \end{bmatrix} \tag{32}$$

where S_i =1 if u_i is prescribed
=0 if u_i is not prescribed.

$\boldsymbol{D}$ is a matrix that corresponds to the constitutive equation. For plane stress, it is given by

$$\boldsymbol{D} = \frac{E}{1-\nu^2}\begin{bmatrix} 1 & \nu & 0 \\ \nu & 1 & 0 \\ 0 & 0 & \dfrac{1-\nu}{2} \end{bmatrix} \tag{33}$$

For plane strain problems, in the above relation E is replaced by $E/(1-\nu^2)$, and ν by $\nu/(1-\nu)$.

In evaluating the $[\boldsymbol{K}]$ the effective Poisson's ratio and effective Young's modulus should be introduced appropriately, depending upon whether the material point is in the elastic state or the elasto-plastic state. In Eq. (28) for the stiffness matrix, the constitutive relation is changed from $\boldsymbol{D}$ matrix to $\boldsymbol{D_{eff}}$ matrix, which is obtained from Eq. (6) using the material parameters E_{eff} and υ_{eff}. The stiffness matrix can be written as

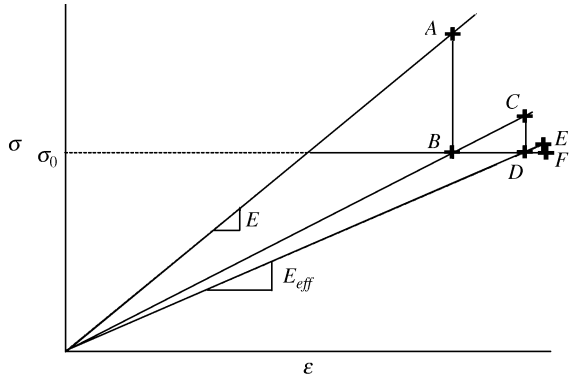

Fig. 1 Projection method

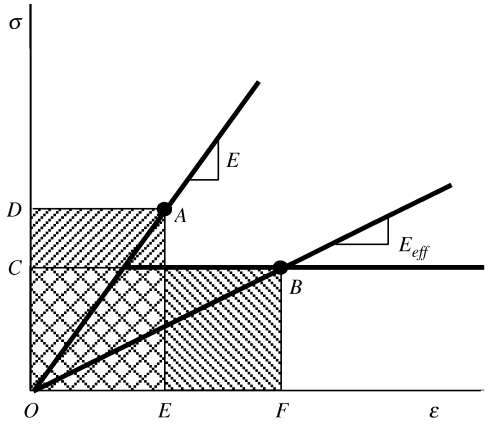

Fig. 2 Neuber's method

$$\boldsymbol{K} = \int_{\Omega} \boldsymbol{B}^T \boldsymbol{D}_{\boldsymbol{eff}} \boldsymbol{B} d\Omega + \lambda \int_{\Gamma_2} \boldsymbol{H}^T \boldsymbol{S} \boldsymbol{H} d\Gamma \qquad (34)$$

5. Determination of Effective Parameters

In the present section two methods (Desikan and Sethuraman, 2000), Projection method and Neuber's method, used for the determination of effective material parameters, E_{eff} and υ_{eff}, needed to calculate D_{eff}, are explained briefly.

In the projection method, initially, a linear elastic EFGM analysis is carried out. Consider a particular material point, and evaluate the equivalent stress from linear elastic analysis. The state is shown as a point 'A' in Fig. 1. This point has crossed the yield stress. Keeping the strain values the same, i.e. strain controlled, and projecting the point 'A' on the experimental uniaxial curve (point 'B'), the effective value of Young's modulus for the next iteration is obtained. Substituting this effective value in Eq. (8) the effective Poisson's ratio is obtained. These effective values are obtained for all the nodal and Gauss points, which have been yielded. With this new set of effective material parameters the next linear elastic EFGM analysis is performed. This iterative procedure is repeated and elastic analysis with currently evaluated E_{eff} and υ_{eff} is performed until all the effective material parameters converge and equivalent stress falls on the experimental uniaxial stress-strain curve.

The Neuber method is based on total energy balance (strain energy and complementary energy). This method assumes that the total energy density evaluated using hypothetical elastic analysis is equal to the total energy density evaluated using the actual elastic-plastic stress state. Consider that the yielded point 'A', which is obtained initially from linear elastic analysis, as shown in Fig. 2, is projected on to the uniaxial curve at the point 'B'. While projecting, the total strain energy is assumed to be conserved i.e., the area ODAEO (hypothetical elastic energy) is the same as area OCBFO (updated elasto-plastic energy). Thus a corresponding point on the uniaxial material curve, which is having the same strain energy, is found out. The equivalent area for the Ramberg-Osgood model has been obtained using the Newton-Raphson technique. With the point on the uniaxial curve, the effective Young's modulus is obtained and is substituted in Eq. (8) to get the effective Poisson's ratio for the next iteration.

III. RESULTS AND DISCUSSION

The effectiveness of the pseudo-elastic analysis based EFGM is illustrated with a problem of a cylindrical vessel under plane strain and plane stress conditions subjected to internal pressure and shear loads. Three different material models are considered for the problem viz: elastic-perfectly plastic, linear strain hardening type and nonlinear behavior obeying Ramberg -Osgood model.

The geometry and the boundary loading conditions are shown in Fig. 3a. The ratio of outer radius to inner radius is 5. The material having Young's modulus 2.0×10^5 MPa, Poisson's ratio 0.3, and yield stress, σ_0, and 200MPa is considered for the analysis. For the elastic linear hardening case, the tangent modulus is taken as one fourth of the Young's modulus. For material obeying the Ramberg-Osgood model, yield offset α=3/7 and hardening exponent n=5 are considered. The penalty parameter, λ, has been chosen from the literature (Zhu and Atluri, 1998). In all the cases the linear basis function has been used in constructing moving least square approximating functions. The results are presented by considering the problem for three loading conditions and are given in the following sections.

1. Cylinder Subjected to Internal Pressure Alone

Initially, a cylinder subjected to internal

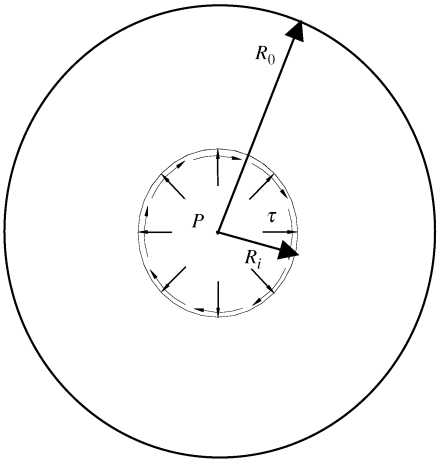

(a)

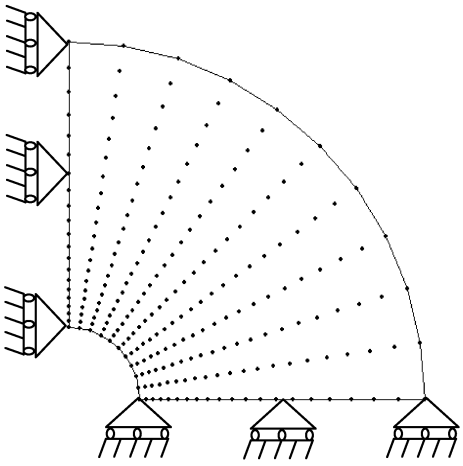

(b)

Fig. 3 (a) Cylindrical pressure vessel subjected to internal surface loading; (b) one quarter model of cylinder with nodal distribution

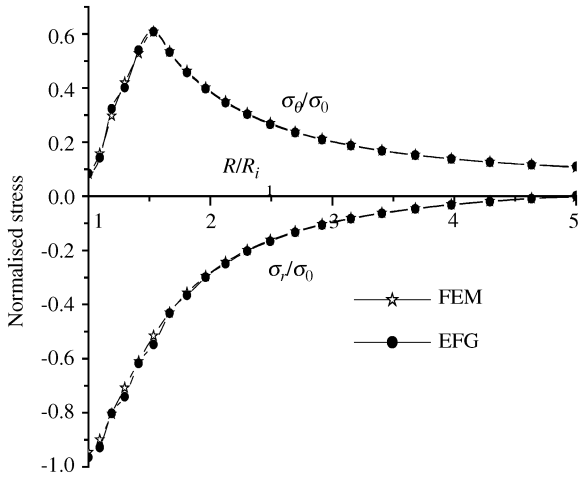

Fig. 4 Normalised stress variation along the radial direction

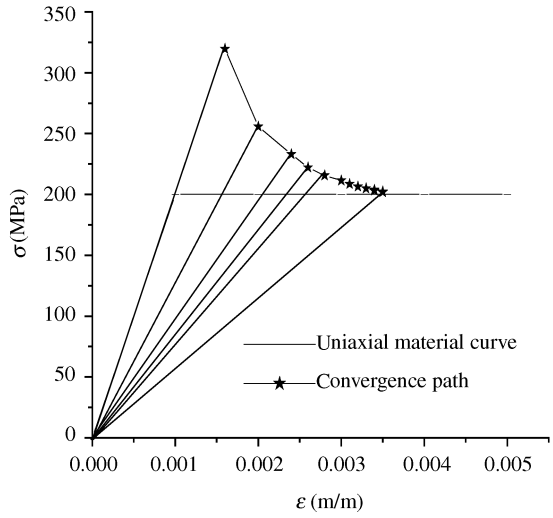

Fig. 5 Convergence path for a particular pseudo elastic point

pressure under plane stress alone is considered. Due to symmetry, only one-quarter of the problem is analysed. The domain is divided into 20 by 10 cells with the nodes coincident with the cell corners. The nodes are equally spaced in the tangential direction while in the radial direction the spacing between two successive nodes is uniformly increased from the interior boundary to the external boundary (Fig. 3b).

At first the results are presented for the elastic-perfectly plastic material model. The radial and hoop stress variations along the thickness direction of the cylinder for pressure ratio 1.0 are shown in Fig. 4. The results are compared with the ANSYS nonlinear finite element results. In all the cases considered for finite element analysis, the number of FEM nodes and elements are same as the EFG nodes and cells respectively. It is observed that the stresses are in good agreement. Fig. 5 shows how a pseudo elastic material point converges and finally falls on the experimental uniaxial curve. Here, convergence is assumed to be achieved when the difference between the material parameters evaluated during consecutive iterations is less than 1% for all the points.

Figure 6 shows the state of stress for all the material points after convergence. It can be seen that in the present method, all the material points fall very close to the uniaxial material curve. Fig. 7 gives the stress variations for different internal pressure ratios.

Figures 8 to 11 gives the results for linear strain hardening material model. Here also note that the results obtained from pseudo elastic analysis based EFGM is in close agreement with finite element results. The convergence based on the projection method and on Neuber's is observed to be very fast in comparison with the elastic-perfectly plastic material case.

For material following the Ramberg-Osgood

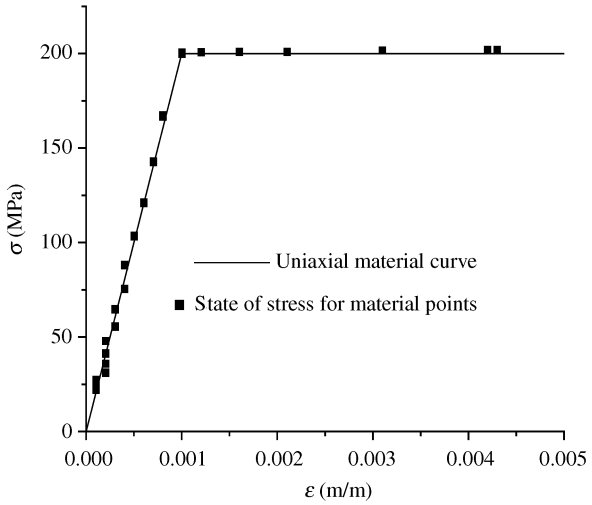

Fig. 6 State of stress for all material points after convergence

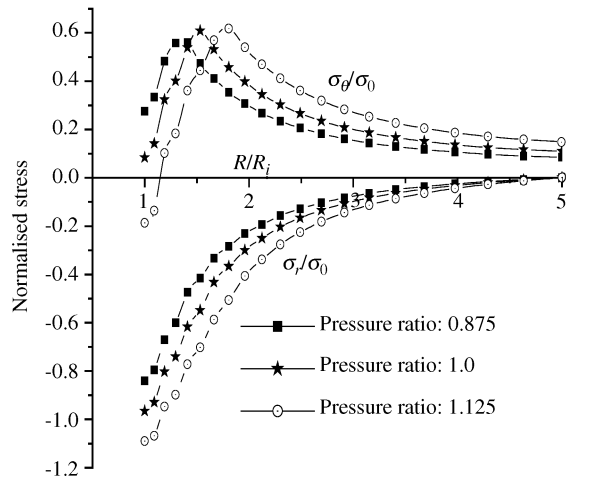

Fig. 7 Normalised stress distribution for different pressure ratios

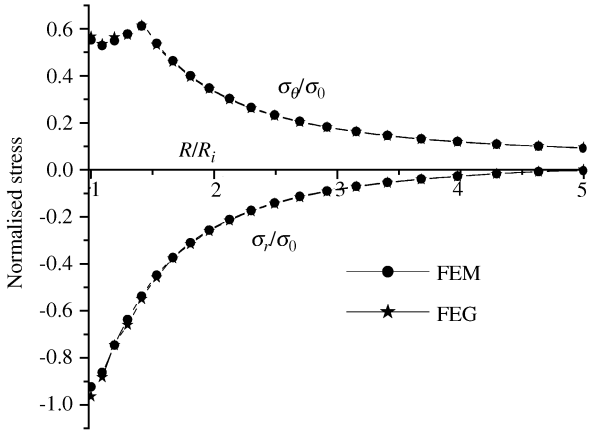

Fig. 8 Normalised stress variation along the radial direction

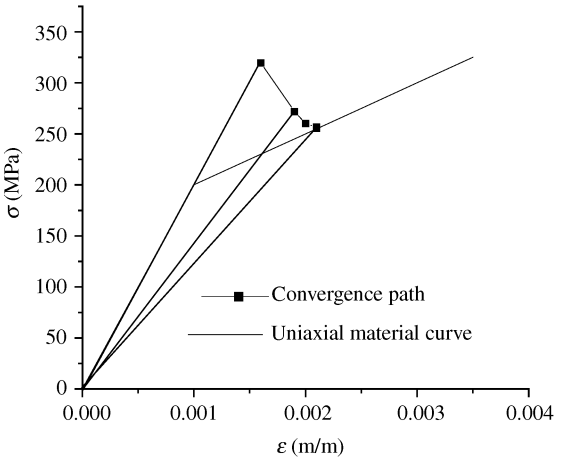

Fig. 9 Convergence path for a particular pseudo elastic point

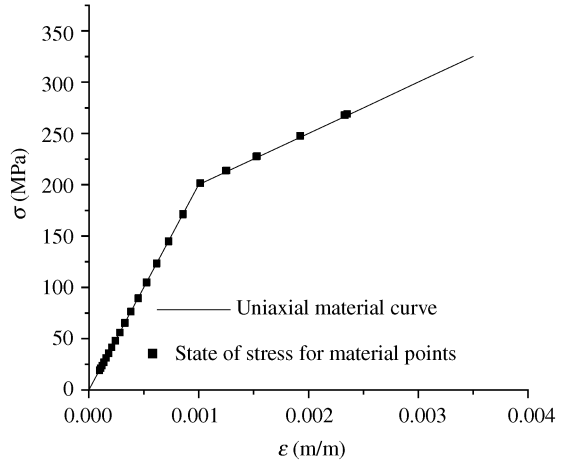

Fig. 10 State of stress for all material points after convergence

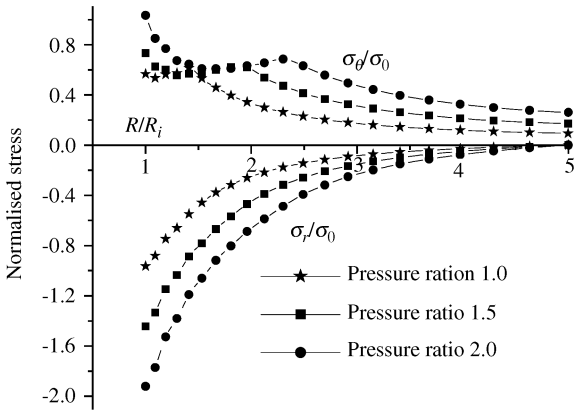

Fig.11 Normalised stress distribution for different pressure ratios

nonlinear behavior the results are shown in Figs. 12-15. When compared with ANSYS, it can be observed that the stresses are in good agreement.

In Table 1 the number of iterations needed for convergence, with a material point to fall on to the uniaxial material curve is shown. It has been observed that, for all the three material types, Neuber's method

Table 1 Number of iterations for convergence

	Elastic-perfectly plastic			Linear strain hardening			Ramberg-Osgood model		
Pressure ratio	0.875	1.0	1.125	1.0	1.5	2.0	1.0	1.5	2.0
No. of iterations in projection method	9	13	27	5	6	6	6	9	12
No. of iterations in Neuber's method	6	9	20	4	5	5	4	6	8

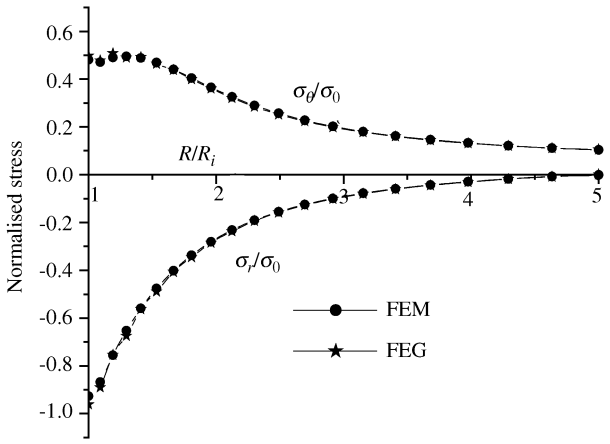

Fig. 12 Normalised stress variation along the radial direction

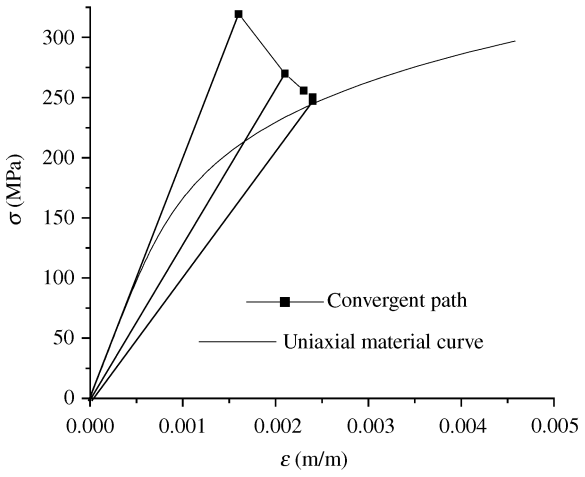

Fig. 13 Convergence path for a particular pseudo elastic point

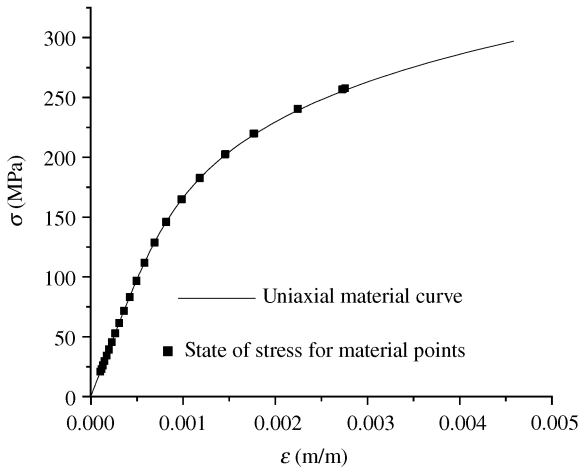

Fig. 14 State of stress for all material points after convergence

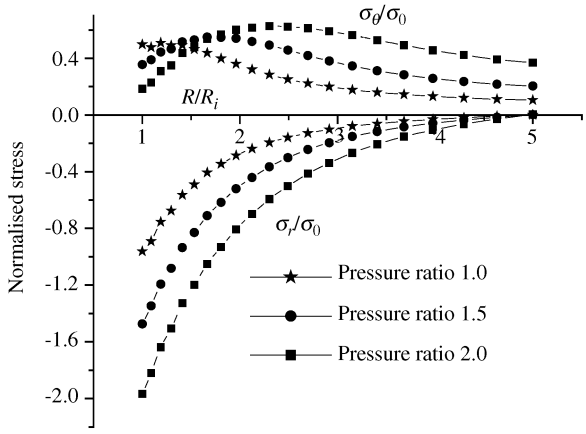

Fig. 15 Normalised stress distribution for different pressure ratios

converges very fast. The fast convergence of Neuber's method is very noticeable for elastic-perfectly plastic material.

2. Cylinder Subjected to Internal Shear Traction Alone

Next a problem of a cylindrical pressure vessel subjected to internal shear traction, τ, under plane stress is considered. The nodal load statically equivalent to shear traction is evaluated with consistent formulation. The material is of von-Mises type and assumed to be characterized by nonlinear behavior obeying the Ramberg-Osgood model with yield offset, α =3/7 and hardening coefficient, n=5. Shear traction of magnitude equal to 200MN/m per unit thickness is applied on the inner surface of the cylinder and all the degrees of freedom at the outer surface

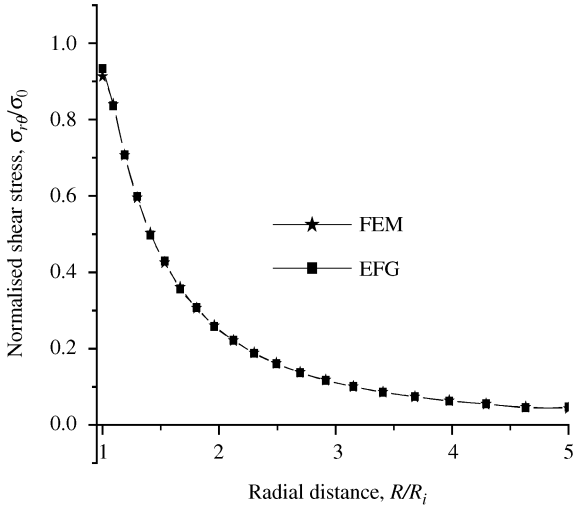

Fig. 16 Normalised shear stress variation along the radial direction

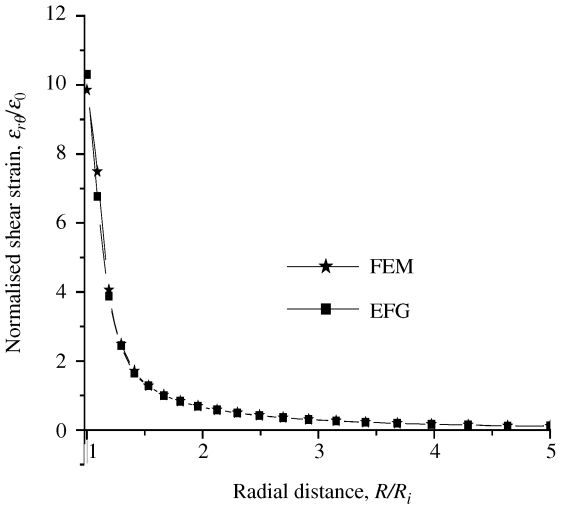

Fig. 17 Normalised shear strain variation along the radial direction

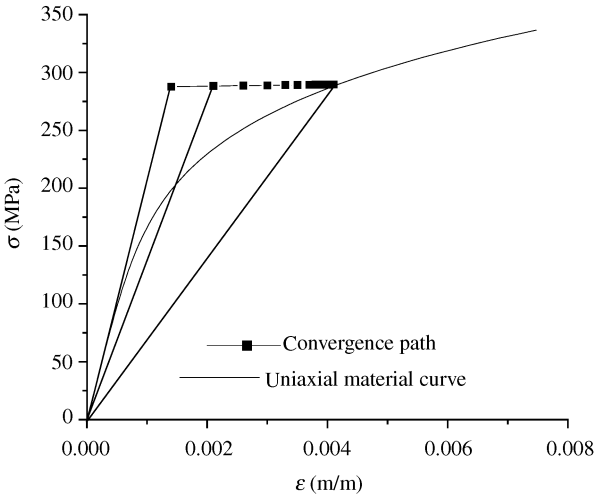

Fig. 18 Convergence path for a particular pseudo elastic point

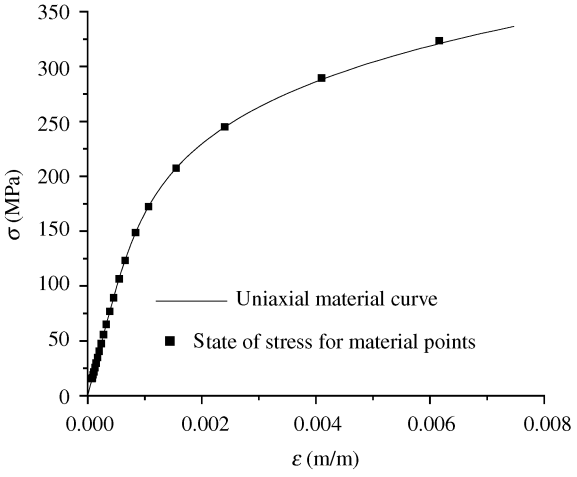

Fig. 19 State of stress for all material points after convergence

are completely fixed.

In Fig. 16, the distribution of the normalized shear stress, $\sigma_{r\theta}/\sigma_0$, along the radial direction is compared with the elasto-plastic finite element results. It is observed that the shear stress distribution obtained from pseudo-elastic analysis based EFGM is in good agreement with the FEM results. In Fig. 17, shear strain, which is normalised, is compared with FEM results and is found to be in very close agreement. The convergence path for a particular material point is shown in Fig. 18. It is interesting to observe that the convergence path for a particular point is a straight line as normal stresses in the radial and tangential directions are always zero i.e. a state of pure shear. For this load case, the number of iterations needed for convergence is 13 for the projection method and 9 for Neuber's method. Again Neuber's method is performing well for the shear traction load case. Fig. 19 shows the state of stress for all the material points after convergence has taken place and also shows that all the material points fall on the uniaxial material curve.

3. Cylinder Subjected to Internal Pressure and Shear Loadings

Finally, a problem of a cylinder subjected to both internal pressure and shear loadings is considered. The full domain is divided into 840 nodes with 40 nodes in the circumferential direction and 21 nodes in the radial direction. These nodes are equally spaced in the tangential direction, while in the radial direction the spacing is uniformly increased. The geometry and loading are shown in Fig. 3a. For the essential boundary conditions, all the degrees of freedom at the outer surface are completely fixed. An

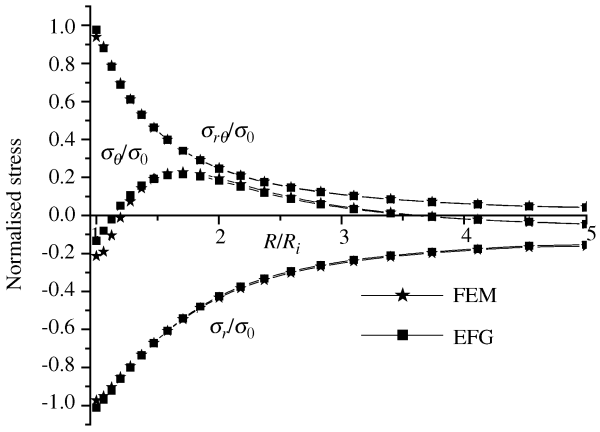

Fig. 20 Normalised stress variation along the radial direction

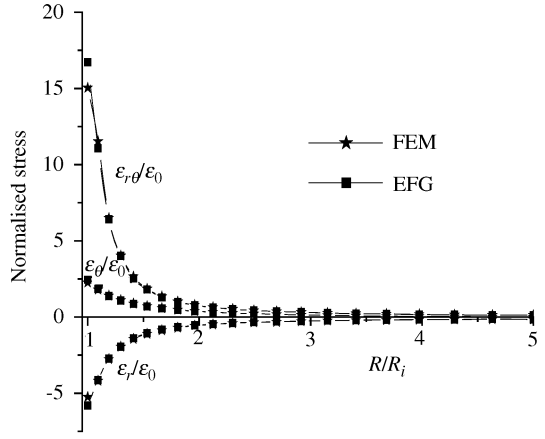

Fig. 21 Normalised strain variation along the radial direction

internal pressure, P, and shear traction, τ, equal to material yield stress, σ_0, is considered for both the considered plane stress and plane strain cases. The results are presented in figures from 20 to 23 for plane stress case and figures from 24 to 27 for plane strain case. It can be observed from Fig. 20 that $\sigma_{r\theta}$ and σ_r is in good agreement with FEM results. The EFGM is estimating higher values for σ_θ in the elasto-plastic region and has good agreement in the elastic region. All the strain components are in good agreement with FEM results.

Only for the combined pressure and shear loadings, it has been observed that, for both plane stress and plane strain cases, the nearer the inner surface the hoop stress component is, the more it deviates from FEM results. We also noticed from the study that there is a substantial improvement in the hoop stress estimation at the inner surface when we have used more nodes at the inner boundary while lumping the traction in a consistent way. But, in the paper results are given for the considered nodal arrangement.

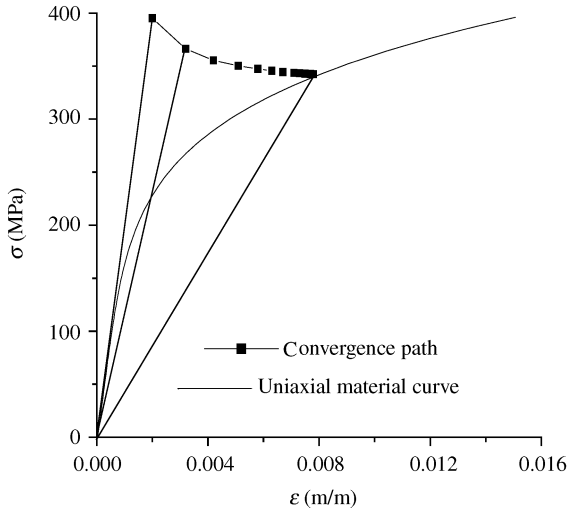

Fig. 22 Convergence path for a particular pseudo elastic point

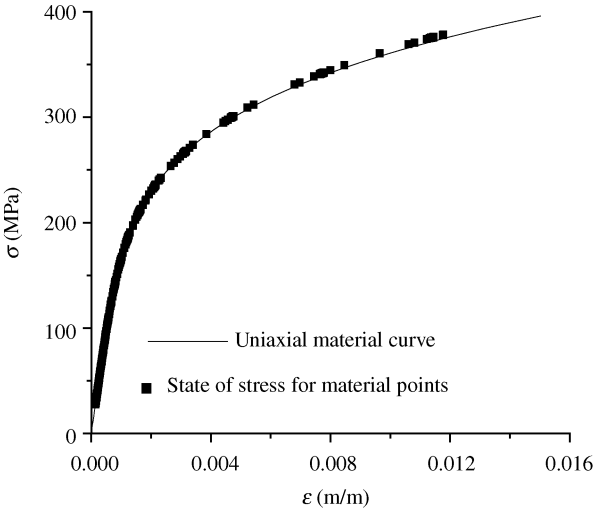

Fig. 23 State of stress for all material points after convergence

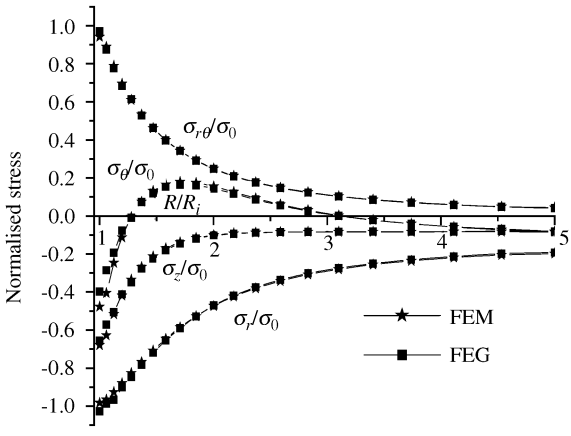

Fig. 24 Normalised stress variation along the radial direction

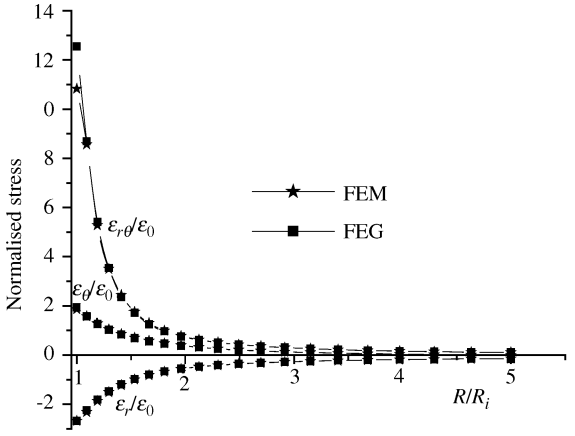

Fig. 25 Normalised strain variation along the radial direction

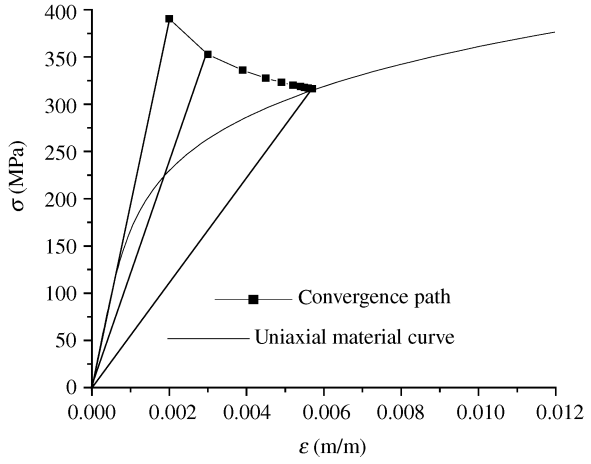

Fig. 26 Convergence path for a particular pseudo elastic point

IV. CONCLUSIONS

Element free Galerkin method based on pseudo elastic analysis is presented for the evaluation of inelastic stress and strain states. The proposed method can be easily adapted to the existing linear elastic EFGM code with suitable updating of elastic material properties with effective material parameters, which are readily obtained in an iterative manner from one-dimensional uniaxial material curve of a given material. Von-Mises material characterized by elastic perfectly plastic, linear work hardening and general hardening obeying Ramberg-Osgood behavior are considered for the problem of a pressure vessel subjected to internal pressure and shear loads. Stress and strain fields obtained for most of the cases are found to be in good agreement with the available nonlinear finite element results.

NOMENCLATURE

b_i	body force vector component

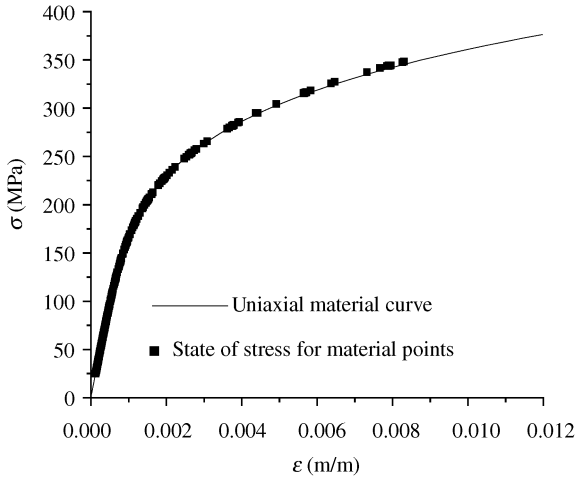

Fig. 27 State of stress for all material points after convergence

$[\boldsymbol{B}]$	strain displacement matrix
$[\boldsymbol{D}]$	constitutive matrix
e	elastic
eff	effective
eq	equivalent
E	Young's modulus
E_T	tangent modulus
E_{eff}	effective Young's modulus
EFGM	Element Free Galerkin Method
$\{\boldsymbol{F}\}$	force vector
FEM	Finite Element Method
i,j,k,m	free and dummy indices used for tensor components
$[\boldsymbol{K}]$	stiffness matrix
MLS	Moving Least Square
n	hardening exponent
p	plastic
P	internal pressure
R_i	inner radius of the pressure vessel
R_0	outer radius of the pressure vessel
S_{ij}	deviatoric stress tensor
t_i	surface traction vector component
u_i	displacement vector component
$\{\overline{\boldsymbol{u}}\}$	prescribed boundary displacement
$\{\hat{\boldsymbol{u}}\}$	nodal displacement vector
w_i	weight function associated with node i
α	yield offset in Ramberg-Osgood model
δ_{ij}	Kronecker delta
ε	experimental uniaxial total strain
ε^p	experimental plastic strain
ε^p_{eq}	equivalent plastic strain
ε_r	radial strain
ε_θ	hoop strain or tangential strain
$\varepsilon_{r\theta}$	shear strain in cylindrical coordinate system
ε_{ij}	strain tensor
Φ	scalar-valued function

φ	shape functions
λ	penalty parameter
ν	Poisson's ratio
ν_{eff}	effective Poisson's ratio
μ	scaling parameter
σ	experimental uniaxial stress
σ_0	yield stress
σ_r	radial stress
σ_θ	hoop stress or tangential stress
$\sigma_{r\theta}$	shear stress in cylindrical coordinate system
σ_{ij}	stress tensor
σ_{eq}	equivalent stress
τ	shear traction

REFERENCES

ANSYS Release 5.6, 1999, *Structural Analysis Guide*, ANYS Inc., Canonsburg, PA, USA.

Babu, S., and Iyer, P. K., 1998, "Inelastic Analysis of Components Using a Modulus Adjustment Scheme," *International Journal of Pressure Vessel and Piping*, Vol. 120, pp. 1-5.

Barry, W., and Saigal, S., 1999, "A Three Dimensional Element Free Galerkin Elastic and Elastic Plastic Formulation," *International Journal for Numerical Methods in Engineering*, Vol. 46, No. 5, pp. 671-693.

Belytschko, T., Krongauz, Y., Organ, D., Fleming, M., and Krysl, P., 1996, "Meshless Methods: An Overview and Recent Developments," *Computational Methods in Applied Mechanics and Engineering*, Vol. 139, Nos. 1-4, pp. 3-47.

Belytschko, T., Lu, Y. Y., and Gu, L., 1994, "Element Free Galerkin Methods," *International Journal for Numerical Methods in Engineering*, Vol. 37, pp. 229-256.

Belytschko, T., Lu, Y. Y., and Gu, L., 1995, "Crack Propagation by Element Free Galerkin Method," *Engineering Fracture Mechanics*, Vol. 51, No. 2, pp. 295-315.

Chen, J. S., Pan, C., Roque, C. M. O. L., and Wang, H. P., 1998 "A Lagrangian Reproducing Kernel Particle Method for Metal Forming Analysis," *Computational Mechanics*, Vol. 22, No. 3, pp. 289-307.

Chen, J. S., Pan, C., Wu, C. T., and Liu, W. K., 1996 "Reproducing Kernel Particle Methods for Large Deformation Analysis of Nonlinear Structures," *Computational Methods in Applied Mechanics and Engineering*, Vol. 139, Nos. 1-4, pp. 195-227.

Desikan, V., and Sethuraman, R., 2000, "Analysis of Material Nonlinear Problems Using Pseudo elastic Finite Element Method," *ASME Trans-action, Journal of Pressure Vessel Technology*, Vol. 122, No. 4, pp. 457-461.

Jahed, H., Sethuraman, R., and Dubey, R. N., 1997, "A Variable Material Property Approach for Solving Elasto-Plastic Problems," *International Journal of Pressure Vessel and Piping*, Vol. 71, No. 3, pp. 285-291.

Lancaster, P., and Salkauskas, K., 1981, "Surfaces Generated by Moving Least Squares Methods," *Mathematics of Computation*, Vol. 37, No. 155, pp. 141-158.

Liu, G. R., 2002, *Mesh Free Methods - Moving beyond Finite Element Method*, CRC Press, Boca Raton, FL, USA.

Lucy, L.B., 1977, "A Numerical Approach to the Testing of the Fission Hypothesis," *The Astronomical Journal*, Vol. 82, No. 12, pp. 1013-1024.

Nayroles, B., Touzat, G., and Villon, P., 1992, "Generalizing the Finite Element Method: Diffuse Approximation and Diffuse Elements," *Computational Mechanics*, Vol. 10, pp. 307-318.

Rao, B. N., and Rahman, S., 2003, "Mesh-Free Analysis of Cracks in Isotropic Functionally Graded Material," *Engineering Fracture Mechanics*, Vol. 70, No. 1, pp. 1-27.

Seshadri, R., and Babu, S., 2000, "Extended GLOSS Method for Determining Inelastic Effects in Mechanical Components and Structures: Isotropic Materials," *ASME Transaction, Journal of Pressure Vessel Technology*, Vol. 122, No. 4, pp. 413-420.

Wang, J. G., Liu, G. R., and Lin, P., 2002, "Numerical Analysis of Biot's Consolidation Process by Radial Point Interpolation Method," *International Journal of Solids and Structures*, Vol. 39 , No. 6, pp. 1557-1573.

Xu, Y., and Saigal, S., 1999, "An Element Free Galerkin Analysis of Steady Dynamic Growth of a Mode I Crack in Elastic-Plastic Material," *International Journal of Solids and Structures*, Vol. 36, No. 7, pp. 1045-1079.

Zhu, T., and Atluri, S. N., 1998, "A Modified Collocation Method and a Penalty Formulation for Enforcing the Essential Boundary Conditions in the EFGM," *Computational Mechanics*, Vol. 21, No. 3, pp. 211-222.

Manuscript Received: Jul. 01, 2003
Revision Received: Feb. 26, 2004
and Accepted: Jan. 27, 2004